Structure, Exchange Determinants, and Family-Wide Rab Specificity of the Tandem Helical Bundle and Vps9 Domains of Rabex-5

Anna Delprato, Eric Merithew,
and David G. Lambright*
Program in Molecular Medicine
and Department of Biochemistry and Molecular
    Pharmacology
University of Massachusetts Medical School
Worcester, Massachusetts 01605

Summary

The Rab5 GTPase, an essential regulator of endocytosis and endosome biogenesis, is activated by guanine-nucleotide exchange factors (GEFs) that contain a Vps9 domain. Here, we show that the catalytic core of the Rab GEF Rabex-5 has a tandem architecture consisting of a Vps9 domain stabilized by an indispensable helical bundle. A family-wide analysis of Rab specificity demonstrates high selectivity for Rab5 subfamily GTPases. Conserved exchange determinants map to a common surface of the Vps9 domain, which recognizes invariant aromatic residues in the switch regions of Rab GTPases and selects for the Rab5 subfamily by requiring a small nonacidic residue preceding a critical phenylalanine in the switch I region. These and other observations reveal unexpected similarity with the Arf exchange site in the Sec7 domain.

Introduction

As regulators of membrane trafficking, Rab proteins comprise the largest GTPase family with at least 38 functionally distinct proteins and 20 isoforms in the human genome (Pereira-Leal and Seabra, 2001; Pfeffer, 2001; Segev, 2001; Zerial and McBride, 2001). The localization and cycling of Rab GTPases between active (GTP bound) and inactive (GDP bound) conformations depends on accessory factors that modulate membrane association, nucleotide binding, and GTP hydrolysis. Upon targeting to donor membranes, Rab GTPases are activated by guanine nucleotide exchange factors (GEFs) and subsequently interact with diverse effectors to facilitate vesicle budding, cargo sorting, and motor-dependent transport as well as the tethering, docking, and fusion of vesicles with acceptor membranes. GTP hydrolysis accelerated by GTPase-activating proteins (GAPs) completes the cycle, allowing recovery of prenylated Rab GTPases as a soluble complex with Rab GDI (GDP-dissociation inhibitor).

Rab5 has been implicated as a master regulator of endocytic trafficking. The function of Rab5 in endosome fusion is mediated by several effectors, including the tethering factor EEA1 and the divalent effectors Rabaptin-5 and Rabenosyn-5, which possess separate binding sites for Rab5 and Rab4 (Christoforidis et al., 1999; de Renzis et al., 2002; Gournier et al., 1998; Lippe et al., 2001; Merithew et al., 2003; Mills et al., 1998; Nielsen et

al., 2000; Simonsen et al., 1998; Stenmark et al., 1995). Rabex-5 (Rabaptin-5 associated exchange factor for Rab5) was identified as a 60 kDa protein that copurified as a stable endogenous complex with Rabaptin-5 (Horiuchi et al., 1997). The Rabex-5-Rabaptin-5 complex catalyzes nucleotide exchange for Rab5 and cooperates with other factors to promote endosome fusion (Gournier et al., 1998; Horiuchi et al., 1997; Lippe et al., 2001; McBride et al., 1999). Rabex-5 contains a central region homologous to the yeast protein Vps9p (Burd et al., 1996; Horiuchi et al., 1997). Null and temperature sensitive mutations in the Vps9 gene result in enlarged vacuoles and improper sorting of vacuolar proteins (Burd et al., 1996).

The Vps9 domain is conserved in 18 mammalian proteins, including Rabex-5, the RIN (*R*as *I*nteraction/*In*terference) family of Ras effectors, and the ALS2 (Amyotrophic Lateral Sclerosis Type 2) protein (Bateman et al., 2004; Letunic et al., 2004). The Vps9p, RIN, and ALS2 proteins catalyze nucleotide exchange for Rab5 or the yeast homolog Vps21p (Esters et al., 2001; Hama et al., 1999; Kajiho et al., 2003; Otomo et al., 2003; Tall et al., 2001). The RIN proteins contain Ras association domains that facilitate allosteric regulation of Rab5 exchange activity by GTP bound Ras (Han et al., 1997; Tall et al., 2001; Wang et al., 2002). RIN1 knockout mice exhibit enhanced long-term potentiation in the amygdala and increased formation of aversive memories (Dhaka et al., 2003). RIN1 also associates with the BCR-ABL fusion protein, potentiates the oncogenic activity of BCR-ABL in hematopoietic cells, and accelerates BCR-ABL-induced leukemia in mice (Afar et al., 1997; Han et al., 1997). The ALS2 protein contains a Dbl homology-pleckstrin homology (DH-PH) tandem, several MORN repeats, and a C-terminal Vps9 domain. A number of single nucleotide polymorphisms (SNPs) in the *ALS2* gene have been identified in individuals with an autosomal recessive juvenile-onset syndrome related to ALS. The known SNPs, including one in an exon encoding part of the Vps9 domain, result in truncation of the ALS2 protein (Devon et al., 2003; Eymard-Pierre et al., 2002; Gros-Louis et al., 2003; Hadano et al., 2001; Yang et al., 2001).

The exchange activity of full-length Rabex-5 is weak compared with GEFs for other GTPases, although it is enhanced in the complex with Rabaptin-5 (Esters et al., 2001; Lippe et al., 2001). Whether the weak activity of full-length Rabex-5 reflects autoinhibition or is an inherent property of the catalytic domain remains to be investigated. Furthermore, some GEFs, notably those for Arf and Rho GTPases, have overlapping specificities for one or more members of their respective GTPase families (Cerione and Zheng, 1996; Macia et al., 2001; Whitehead et al., 1997). However, the specificity of mammalian Rab GEFs has not been systematically characterized, owing to the size and phylogenetic complexity of the Rab family.

To gain insight into Rab recognition by Vps9 domains, we have identified a region of Rabex-5 with robust GEF activity, determined the crystal structure, and analyzed

*Correspondence: david.lambright@umassmed.edu
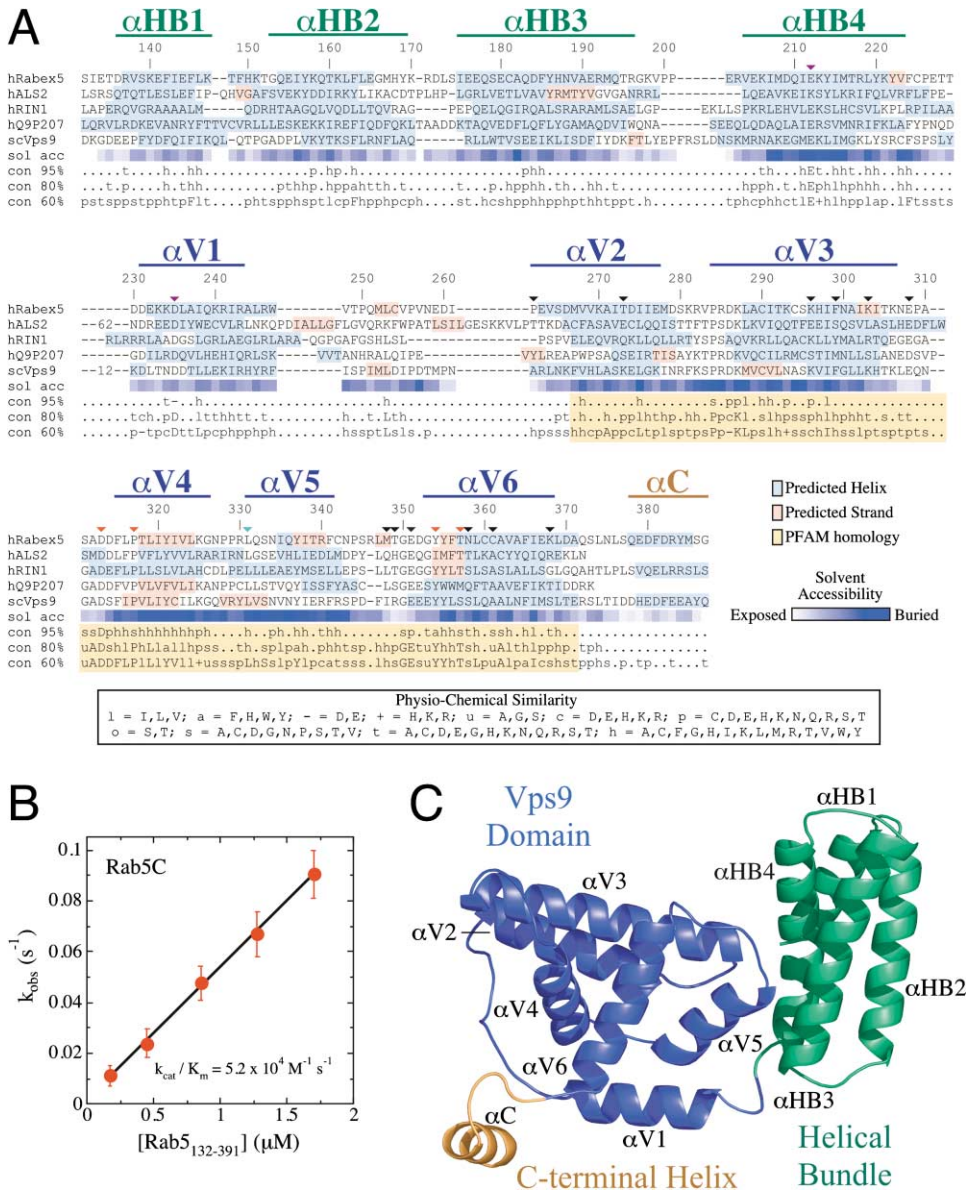
Figure 1. Structure and Kinetic Properties of the Rabex-5 Catalytic Core

(A) Structure-based alignment of representative Vps9 domain proteins. Residue numbers and observed secondary structure for Rabex-5 are shown above the alignment. Predicted helices, strands, and the SMART/PFAM Vps9 homology region are highlighted in blue, orange, and yellow, respectively. Fractional solvent accessibility (sol acc) for each residue in Rabex-5 is indicated as a box with a gradient from exposed (light blue) to buried (dark blue). The consensus of physiochemical similarity in an alignment of 20 sequences (Supplemental Figure S1 available on *Cell* website) is shown at conservation levels of 60% (con 60%), 80% (con 80%), and 95% (con 95%).

(B) Observed rate constant for the exchange of GDP for GppNHp on Rab5 as a function of the concentration of Rabex-5$_{132-391}$. The large change in the intrinsic tryptophan emission of Rab5 accompanying nucleotide exchange was continuously monitored at 340 nm with excitation at 300 nm.

(C) Overall fold and domain organization of Rabex-5$_{132-394}$. The designation of domain boundaries is discussed in the text.

the specificity for the Rab family. The catalytic core of Rabex-5 exhibits high specificity for the Rab5 subfamily and has a tandem architecture in which the Vps9 domain is stabilized by an essential helical bundle. Conserved exchange determinants in the Vps9 domain map to a pair of adjacent helices that resembles the Arf binding site in the Sec7 domain. An analogous mode of interaction is strongly supported by a systematic analysis of specificity determinants, which reveal how the Vps9

domain achieves highly selective recognition of the Rab5 subfamily.

Results

A Core Catalytic Region of Rabex-5 with High Exchange Activity

Rabex-5 has an evolutionarily conserved architecture with an N-terminal Zn^{2+} finger, a Vps9 domain, a heptad

Table 1. Structure Determination and Refinement

Data Collection[a]

Crystal	Se 1	Se 1	Se 1	Se 2	Se 2	Se 2
Wavelength (Å)	λ1 (0.97956)	λ2 (0.97944)	λ3 (0.96805)	λ1 (0.97954)	λ2 (0.97948)	λ4 (0.99530)
Resolution (Å)	20–2.6	20–2.6	20–2.5	20–2.8	20–2.5	20–2.35
R_{sym}(%)[b]	7.5 (35.6)	6.5 (42.7)	7.0 (31.0)	6.9 (33.5)	6.9 (35.1)	5.9 (37.2)
$<I/\sigma>$	22 (2.7)	25 (2.8)	20.3 (2.9)	24.5 (3.9)	28.4 (3.4)	23.3 (2.0)
Completeness (%)	98.1 (94.9)	97.8 (91.8)	97.0 (94.0)	100 (100)	99.9 (100)	96.3 (74.5)
Redundancy	4	4	4	4	4	4

Phasing Power and FOM (Bijvoet Differences)[a]

	Se 1 λ1	Se 1 λ2	Se 1 λ3	Se2 λ1	Se2 λ2
Acentric PP	1.4 (0.51)	1.6 (0.52)	1.5 (0.47)	1.5 (0.54)	1.5 (0.48)

Phasing Power and FOM (Dispersive Differences)[a]

	Se 1 λ1 versus. Se 2 λ4	Se 1 λ2 versus. Se 2 λ4	Se 1 λ3 versus. Se 2 λ4	Se2 λ1 versus. Se 2 λ4	Se2 λ2 versus. Se 2 λ4
Acentric PP	1.3 (0.88)	1.3 (0.90)	0.48 (0.32)	1.7 (1.2)	1.9 (0.87)
Centric PP	1.04 (0.65)	1.04 (0.72)	0.4 (0.25)	1.2 (0.74)	1.4 (0.76)
Acentic FOM	0.59 (0.16)				
Centric FOM	0.53 (0.19)				

Refinement

			RMS Deviations	
Resolution (Å)	R Factor (%)	R_{free}[c] (%)	Bond Length (Å)	Bond Angle
20–2.35	22.7	26.9	0.006	1.1°

[a] Values in parentheses represent the highest resolution shell.
[b] $R_{sym} = \Sigma_h\Sigma_j|I_j(h) - <I(h)>|/\Sigma_h\Sigma_jI_j(h)$.
[c] R-value for a 5% subset of reflections selected at random and omitted from refinement.

repeat, and a proline rich C terminus. Homologous sequences flanking the Vps9 domain were detected in an alignment of diverse Vps9 domain proteins (Figure 1A and Supplemental Figure S1 available at http://www.cell.com/cgi/content/full/118/5/607/DC1). A Rabex-5 construct consisting of residues 132–391, which includes five predicted helices N-terminal to the Vps9 domain and one on the C-terminal side, expresses at high levels, behaves as a uniform monomer, and exhibits potent exchange activity for Rab5 (Figure 1B). The observed rate constant (k_{obs}) depends linearly on the concentration of Rabex-5$_{132–391}$ to at least 2 μM, requiring lower limits on the apparent Michaelis-Menten kinetic constants such that $k_{cat} > 0.1$ s^{-1} and $K_m > 2$ μM. Constructs that truncate predicted helices at the N- or C terminus express poorly and/or are prone to aggregation. Consistent with this observation, Rabex-5$_{132–391}$ resists proteolysis by LysC, GluC, ArgC, and chymotrypsin (data not shown). We therefore conclude that the 260 aa helical region encompassing the Vps9 domain represents the catalytic core.

Tandem Architecture of the Catalytic Core

The structure of selenomethionine-substituted Rabex-5$_{132–394}$ was solved by multiwavelength anomalous diffraction and refined to 2.35 Å (Table 1). As illustrated in Figure 1C, the catalytic core consists of an N-terminal helical bundle (HB) and the Vps9 domain, which has a novel α helical fold. Helices αHB2-αHB4 in the helical bundle form a triple-stranded antiparallel coiled coil with a right-handed superhelical pitch. The subdomain corresponding to the SMART/PFAM Vps9 homology region adopts a layered fold in which a helical hairpin formed

by αV2 and αV3 supports a middle layer consisting of αV4 and αV5. The N terminus of αV6 packs against the central portion of αV3, allowing the C terminus of αV6 to thread a V-shaped groove between αV4 and αV5.

Although a short helix following αV6 packs against the Vps9 domain and is required for soluble expression, two observations indicate that this helix (αC1) is not a generally conserved element: (1) the similarity following the Vps9 domain is weak; and (2) the C-terminal location of the Vps9 domain in the ALS2 and Q9P207 proteins precludes an analogous helix. In contrast, significant similarity is evident in the sequences N-terminal to the SMART/PFAM homology region (Figure 1 and Supplemental Figure S1 available on *Cell* website). This region encodes an amphipathic helix (αV1) followed by an ordered stretch of random coil. The nonpolar surface of αV1 rests in a hydrophobic groove formed by the C terminus of αV6 and the connecting segment between αV4 and αV5. Likewise, nonpolar residues in the ordered coil following αV1 pack against nonpolar residues from αV4. Given the physiochemical similarity of the residues that lie within these interfaces, we conclude that the Vps9 domain begins with αV1 and terminates with αV6.

In the extensive interface between the HB and Vps9 domains, which buries 1940 Å^2 of surface area, residues from one side of αHB4 pack in a shallow groove between αV5 and the αV2/αV3 loop. A solvent excluded hydrogen bond between the buried carboxylate group of a conserved glutamate residue in αHB4 (Glu 212) and the main chain NH group of Arg 285 at the N terminus of αV3 is enhanced by the favorable disposition of the negatively charged Glu 212 side chain with respect to the positive end of the αV3 helix dipole. An analogous

A

Rab5

Rab21

Rab22

Rab6

| Intrinsic | 0.1 μM Rabex | 1.0 μM Rabex |
| 0.02 μM Rabex | 0.5 μM Rabex | 5.0 mM EDTA |

B

Rab21

Rab5

Rab22

Substrate	k_{cat}/K_m (M⁻¹s⁻¹)	k_{intr} (s⁻¹)
Rab5	2.3×10^4	4×10^{-5}
Rab21	3.2×10^4	9×10^{-5}
Rab22	3.5×10^2	4×10^{-5}
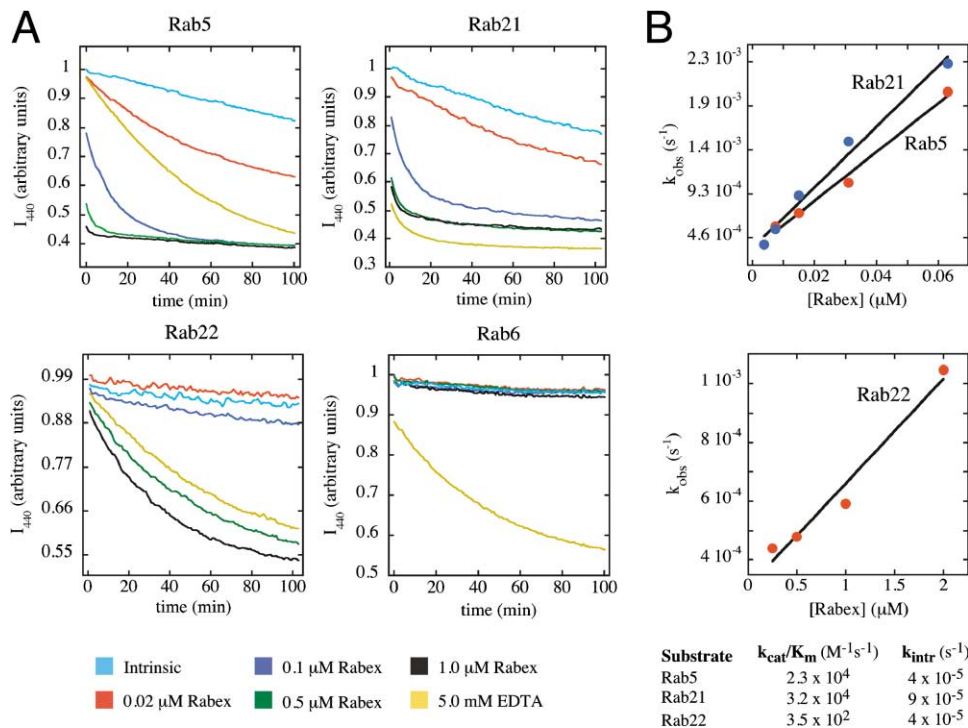
Figure 2. Family-Wide Analysis of Rab Specificity

(A) Kinetics of mant-GDP release from GST-fusions of Rab5, Rab21, Rab22, and Rab6 in the absence (light blue) and presence of 0.02 μM (red), 0.1 μM (dark blue), 0.5 μM (green), and 1 μM (black) Rabex-5$_{132-391}$ or following addition of 5 mM EDTA (yellow). See Figure 2 of the Supplemental Data (available on *Cell* website) for the results of equivalent kinetic experiments for other Rab GTPases.
(B) Dependence of the observed rate constant for mant-GDP release on the concentration of Rabex-5$_{132-391}$.

interaction occurs between the carboxylate group of Asp 235 in αV1 and the main chain NH and side chain hydroxyl groups of Ser 333 at the N terminus of αV5. Substitution of either acidic residue with alanine results in mutant proteins that do not express in a soluble form.

The HB-Vps9 Tandem of Rabex-5 Has High Specificity for the Rab5 Subfamily
To characterize the specificity of effectors and regulatory factors, we have constructed a panel of 37 mammalian Rab GTPases, representing the known Rab family excluding isoforms. The majority (32 Rab GTPases) express in a soluble form with GST fused to the N terminus. Three Rab GTPases (Rab8, Rab10, and Rab17) that are not soluble as GST-fusions express in a soluble form with NusA as an N-terminal fusion partner. Two Rab GTPases (Rab36 and Rab37) do not express in a soluble form as either GST or NusA fusions. The fusion-proteins were purified to >95% homogeneity as determined by SDS-PAGE. With the exception of Rab10, Rab17, Rab26, and Rab28, the soluble Rab GTPases exhibited intrinsic nucleotide exchange and GTP hydrolysis properties characteristic of a functional state.

An established approach for measuring the kinetics of nucleotide release from monomeric GTPases, including Rab GTPases, takes advantage of mant-GDP, which has a fluorescent N-methylanthraniloyl label attached to the 2′- and/or 3′-hydroxyl group (Alexandrov et al., 2001; Nuoffer et al., 1997; Simon et al., 1996; Zhu et al., 2001).

The ability of Rabex-5$_{132-391}$ to catalyze release of mant-GDP from 31 Rab GTPases was determined using a quantitative microplate assay (Figure 2 and Supplemental Figure S2 available on *Cell* website). Under the conditions of these experiments, in which the concentration of Rabex-5$_{132-391}$ is varied from 20 nM to 1 μM, measurable activity is observed for Rab5, Rab21, and Rab22. Addition of 5 mM EDTA, which reduces the free Mg²⁺ concentration to submicromolar levels, greatly stimulates the rate of nucleotide release, indicating that the absence of detectable activity is not due to an inability to release GDP-mant but instead reflects the high specificity of Rabex-5$_{132-391}$.

For the three Rab GTPases that exhibited GEF-stimulated nucleotide release in the initial screen, more detailed kinetic experiments were conducted. Whereas the catalytic efficiency (k_{cat}/K_m) of Rabex-5$_{132-391}$ for Rab5 and Rab21 is indistinguishable, it is 100-fold lower for Rab22. Given the signal-to-noise of the experiments and the readily detectable activity for Rab22, we conservatively estimate that $k_{cat}/K_m < 100$ M⁻¹ s⁻¹ for the other Rab GTPases examined in this study. Interestingly, a phylogenetic analysis of Rab GTPases from diverse organisms identified several distinct subfamilies, one of which consists of Rab5, Rab21, and Rab22 (Pereira-Leal and Seabra, 2000; Pereira-Leal and Seabra, 2001). Thus, the HB-Vps9 tandem of Rabex-5 selectively recognizes the Rab5 subfamily and further distinguishes Rab5 and Rab21 from Rab22.
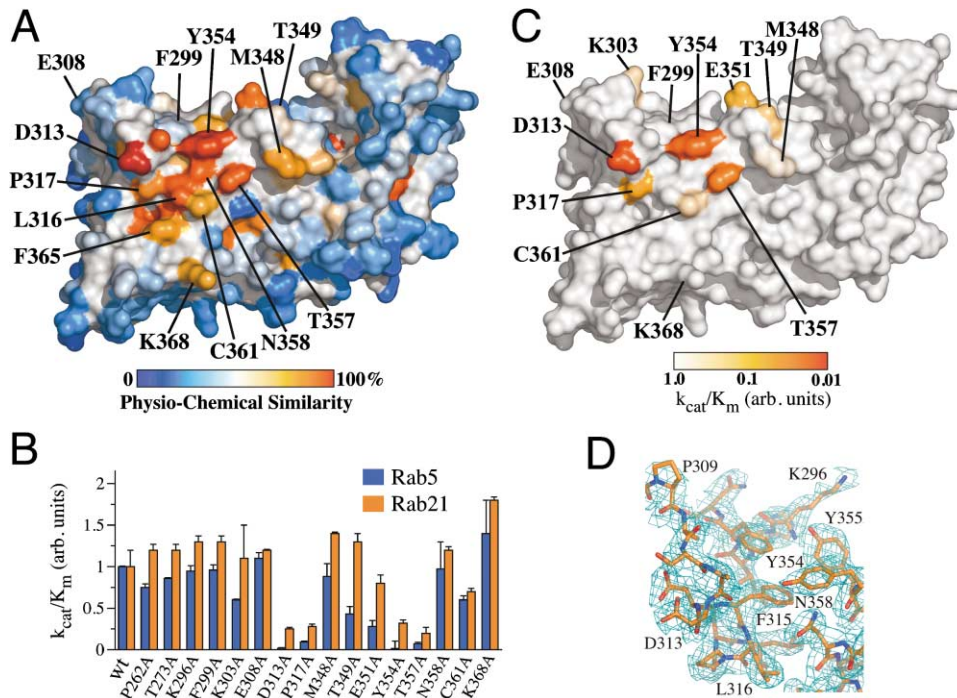
Figure 3. Critical Exchange Determinants Map to a Conserved Surface of the Vps9 Domain

(A) The conservation of physiochemical similarity in an alignment of 20 Vps9 domain proteins (Supplemental Figure S1 available on *Cell* website) was mapped onto the surface of Rabex-5$_{132-394}$. The view is oriented as in Figure 1C.

(B) The catalytic efficiency (k_{cat}/K_m) of mutant and wild-type (wt) Rabex-5$_{132-391}$ was determined for GST fusions of Rab5 and Rab21.

(C) Mutated residues are colored according to the k_{cat}/K_m for mutant and wild-type Rabex-5$_{132-391}$ with GST-Rab5 as the substrate.

(D) Representative region of the experimental map following phase improvement by solvent flipping. The density contoured at 1.0 σ is shown with the final refined model.

A Conserved Surface of the Vps9 Domain Is Critical for GEF Activity

A number of exposed residues in the Rabex-5$_{132-394}$ structure are conserved in diverse Vps9 domain proteins. The majority of these residues cluster on a common surface of the Vps9 domain (Figure 3A). Of particular note is an aspartic acid residue (Asp 313) in the ordered αV4/αV5 loop. The side chain of Asp 313, which represents the only invariant residue, is completely solvent exposed and does not engage in intramolecular interactions. Intriguingly, Asp 313 is situated immediately adjacent to a shallow hydrophobic groove formed by residues from αV4 and αV5. A small number of conserved residues located on the opposite surface are generally more buried and therefore likely to be conserved for structural stability.

To identify determinants of GEF activity, conserved residues with substantial solvent exposure were substituted with alanine. All of the mutant proteins express in a soluble form at wild-type levels and are well behaved. The ability of the Rabex-5$_{132-391}$ mutants to catalyze release of mant-GDP was determined for both Rab5 and Rab21 (Figures 3B and 3C). Mutation of four residues (Asp 313, Pro 317, Tyr 354, and Thr 357) that cluster near the N termini of αV4 and αV6 severely impairs catalytic efficiency. Mutation of two residues flanking the critical cluster (Thr 349 and Glu 351) results in moderate defects whereas mutation of other residues has minimal effect.

Given that the severity of the defects correlates with both conservation and solvent exposure, the simplest interpretation is that the contiguous surface formed by conserved residues from αV4, αV6, and the loops N-terminal to these helices corresponds to the overlapping interaction epitopes for Rab5 and Rab21. Differences in the magnitude of the defects for Rab5 and Rab21 indicate that the mode of interaction, though likely similar, is not identical.

Determinants for Recognition of Rab5 Subfamily GTPases

The Rab5 motifs [53]TIGAAFLT[60] in the switch I region and [83]YHSLAPMY[90] in the switch II region contain three aromatic residues (Phe 58, Tyr 83, and Tyr 90) that are conserved throughout the Rab family as well as several residues that are conserved within the Rab5 subfamily but are strikingly dissimilar in other Rab GTPases (Figure 4). Substitution of Phe 58 or Tyr 83 in Rab5 with alanine severely impairs the ability of Rabex-5$_{132-391}$ to catalyze exchange, despite little or no effect on the intrinsic rates. To test the hypothesis that the switch I and II regions play a key role in specificity determination, residues that are selectively conserved in the Rab5 subfamily were substituted with the consensus residue from the set of Rab GTPases that are not substrates. Although small differences (∼2-fold) are observed for most substitutions, two result in 5-fold lower k_{cat}/K_m (L59K and P88S),
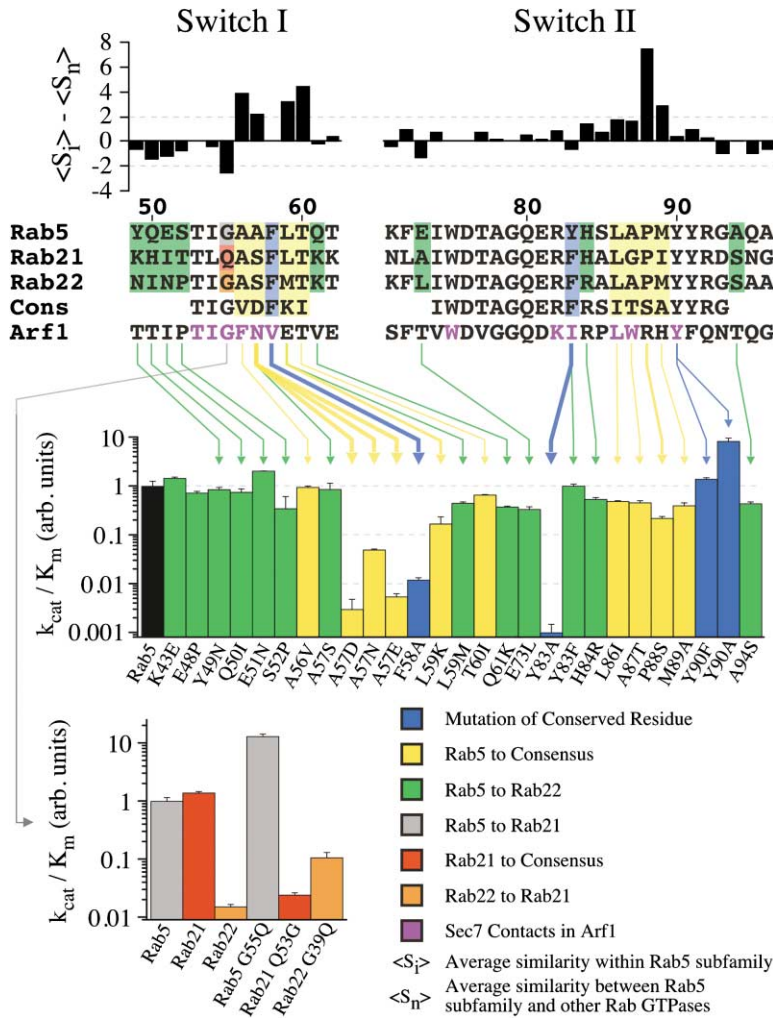
Figure 4. Recognition and Specificity Determinants in Rab5 Subfamily GTPases

The sequences of Rab5 subfamily GTPases within or proximal to the switch I and II regions are compared with the consensus sequence for other Rab GTPases. Shown above the alignment is a log-odds measure of the average similarity within the "interacting set" of Rab GTPases ($<S_i>$) compared to that between the interacting and noninteracting sets ($<S_n>$). Log-odds scores for individual amino acid substitutions were obtained from the Blosum 62 substitution matrix. Positive values reflect lower similarity between the interacting and noninteracting sets whereas negative values reflect lower similarity within the interacting set. Potential determinants of Rab family recognition (blue), selectivity for Rab5 subfamily GTPases (yellow), or variation within the Rab5 subfamily (green, gray, red, and orange) were substituted as indicated in the legend and assayed for exchange activity with Rabex-5$_{132-391}$.

whereas the A57D, A57E, and A57N substitutions, which exhibit intrinsic rates similar to wild-type Rab5, severely disrupt exchange activity (k_{cat}/K_m ∼30–300-fold lower). An acidic residue is conserved at this position in 30 Rab GTPases, even though it is exposed in all known Rab structures and does not contribute to nucleotide binding or conformational switching.

With one exception, Rab GTPases conserve a switch I glycine residue corresponding to Gly 55 in Rab5. In Rab21, this residue is replaced by glutamine, a substitution that is expected to disrupt the characteristic interface between the switch I and II regions in the active conformation. Surprisingly, the Q53G substitution in Rab21 reduces k_{cat}/K_m ∼60-fold to a level comparable to Rab 22, whereas the reciprocal mutations in Rab5 and Rab22 increase k_{cat}/K_m by 12-fold and 7-fold, respectively, indicating that the equivalent catalytic efficiency for Rab5 and Rab21 does not reflect identical determinants. Conversely, substitution of residues within or proximal to the switch regions in Rab5 with the corresponding residue in Rab22 suggests that the preference for Rab5 reflects the cumulative contribution of multiple weak determinants.

These observations demonstrate that the HB-Vps9 tandem recognizes Rab GTPases through general deter-

minants (Phe 58 in switch I and Tyr 83 in switch II) that are conserved throughout the Rab family. The switch II tyrosine is broadly conserved in most GTPase families and typically participates in GEF interactions. Conversely, the switch I phenylalanine residue, though invariant in the Rab family, is replaced by dissimilar residues in other GTPases. The HB-Vps9 tandem distinguishes the Rab5 subfamily from other Rab GTPases primarily through a strict requirement for a small nonacidic residue preceding the invariant switch I phenylalanine, with secondary contributions from nonconservative substitutions at other positions. Interestingly, acidic residues at the position corresponding to Ala 57 in Rab5 occur frequently in other GTPase families. Likewise, dissimilar substitutions are typical at the position following the invariant phenylalanine. Thus, the (A/S)-F-(L/M) motif in the switch I region encodes sufficient dissimilarity to distinguish the Rab5 subfamily from other Rab GTPases as well as other GTPase families.

Structural Similarity in the GTPase Binding Sites of Vps9 and Sec7 Domains

Although the fold of the Vps9 domain differs from that of other GEFs, the functionally critical substructure consisting of the αV4 and αV6 helices bears a striking resem-
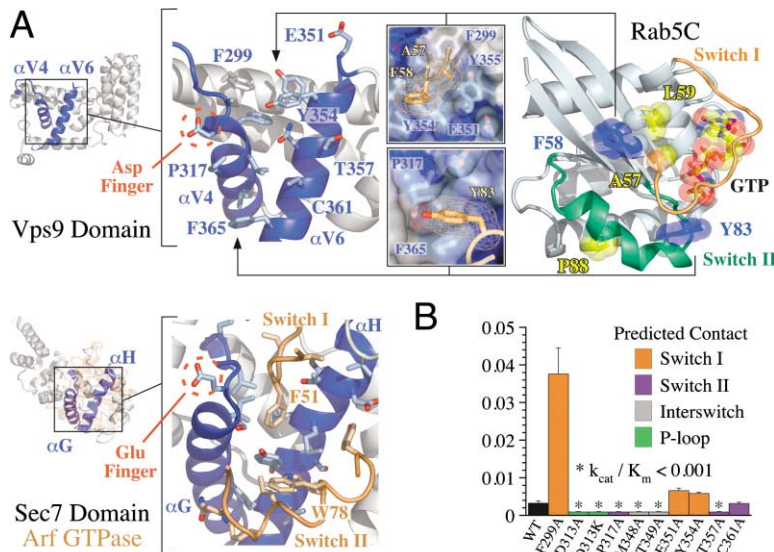
Figure 5. Structural Similarity and Compensatory Effects Support an Overall Mode of Interaction Analogous to the Sec7-Arf Complex

(A) The Rab binding site in the HB-Vps9 tandem of Rabex-5 strongly resembles the Arf binding site in the Sec7 domain of Gea1 from the complex with Arf1•GDP and Brefeldin A (Mossessova et al., 2003). In the Sec7 domain, a pair of helices and adjacent loops (blue) account for the majority of contacts with Arf1 (orange). An analogous pair of helices and adjacent loops in the Vps9 domain contain the conserved exchange determinants. Critical glutamate (Sec7) and aspartate (Vps9) residues are shown in red. Also shown is a model for the Rab5-Vps9 interaction based on the mutational data and the structural similarity of the GTPase binding sites of the Vps9 and Sec7 domains (see text).
(B) Alanine substitutions involving Vps9 residues in the predicted docking site for the [57]A-F-L[59] motif in switch I exhibit selective compensatory effects when combined with the Rab5 A57D mutation.

blance to an analogous substructure in the Sec7 domain that accounts for the majority of the interactions with Arf GTPases (Figure 5A). In the Sec7-Arf1 complexes, the αG and αH helices of the Sec7 domain engage the switch regions of Arf1 such that the phenylalanine residue from a G-F motif in the switch I region docks in a hydrophobic groove between αG and αH whereas residues from the switch II region interact primarily with residues from αG (Mossessova et al., 1998, 2003; Renault et al., 2003). A "glutamate finger" in the loop preceding αG plays a critical role in promoting GDP release and, in the nucleotide free complex, interacts with the invariant lysine residue in the GX₄GK(S/T) motif that encodes the phosphate binding loop (P loop). Like the Sec7 domain, the Vps9 domain contains a hydrophobic groove between the αV4 and αV6 helices as well as an invariant "aspartate finger" in the loop preceding αV4. Both the aspartate finger (Asp 313) and at least one highly conserved aromatic residue in the hydrophobic groove (Tyr 354) are critical determinants of exchange activity.

These observations suggest the intriguing possibility that the Vps9 and Sec7 domains share a similar mode of interaction. Furthermore, the critical switch I (A/S)-F motif in the Rab5 subfamily is strikingly similar to the switch I G-F motif in Arf1 that binds in the hydrophobic groove between the αG and αH helices of the Sec7 domain. We therefore propose that the switch I (A/S)-F motif in the Rab5 subfamily docks in the hydrophobic groove between the αV4 and αV6 helices of the Vps9 domain, explaining the strict requirement for a small nonacidic residue preceding the invariant phenylalanine (Figure 5A, upper inset). Experimental validation for this hypothesis is provided by the observation of robust compensatory effects when alanine mutants that truncate side chains in or near the hydrophobic groove are combined with the A57D mutation in Rab5 (Figure 5B). In particular, the F299A, Y354A, and E351A mutants have catalytic efficiencies for the Rab5 A57D mutant

that are 1–2 orders of magnitude higher than would be expected on the basis of additive free energies, implicating Phe 299, Tyr 354, and Glu 351 as major specificity determinants. In contrast, alanine mutants outside the proposed switch I docking site do not exhibit significant compensatory effects. Moreover, a substantial hydrophobic pocket flanked by Leu 316, Pro 317, and Phe 365 has dimensions appropriate for an aromatic side chain and, assuming an overall orientation similar to that of the Sec7-Arf1 complex, is ideally positioned to accept the aromatic side chain of Tyr 83 in the switch II region of Rab5 (Figure 5A, lower inset).

Although the structural features and mutational analysis support an overall mode of interaction similar to that of Sec7 and Arf1, several observations reveal significant differences. For example, the (A/S)-F motif in the Rab5 subfamily is shifted toward the C terminus of switch I by two residues relative to the G-F motif in Arf1. Likewise, the proposed binding pocket for the critical switch II tyrosine is displaced by a similar magnitude relative to the residues in the Sec7 domain that contact the corresponding residue in Arf1. The invariant aspartate residue is also shifted relative to the glutamate finger. Finally, the D313K charge reversal mutant in the Vps9 domain does not form a stable complex with the GDP bound form of Rab5 (data not shown), in contrast to the corresponding mutation in the Sec7 domain (Renault et al., 2003). These observations suggest that Asp 313, though appropriately positioned to contact the P loop, may not have a functional role that is strictly analogous to the glutamate finger in the Sec7 domain.

A SNP in ALS2 Disrupts the Structure and GEF Function of the Vps9 Domain

One of the SNPs in the *ALS2* gene (4844ΔT) deletes a single base in an exon encoding part of the Vps9 domain (Gros-Louis et al., 2003). This SNP, which generates a frame shift near the N terminus of αV3, replaces the C-terminal half of the Vps9 domain with 43 residues of
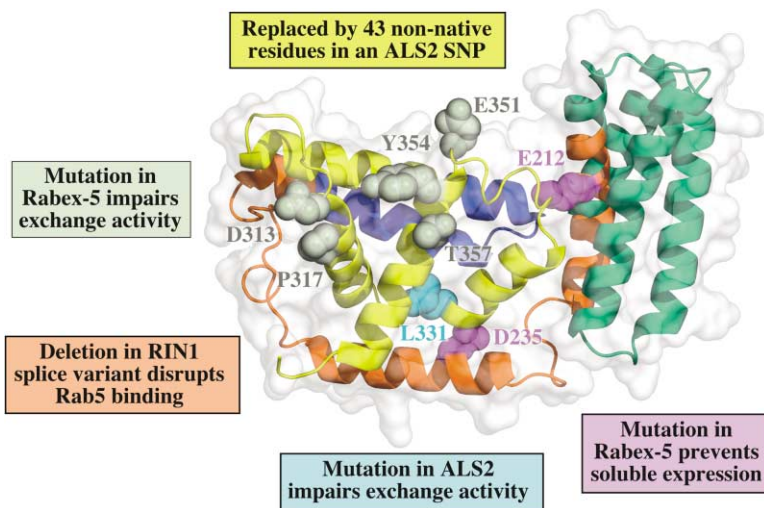
Figure 6. Correlation of Structure and Function in Vps9 Domain Proteins

A SNP in the ALS2 protein replaces the core of the Vps9 domain (yellow), including critical determinants of exchange activity (gray), with 43 residues of nonnative sequence (Gros-Louis et al., 2003). A splice variant of RIN1, which deletes the region from αHB4 to the N terminus of αV1, fails to interact with Rab5 (Tall et al., 2001). Mutation of buried acidic residues in the corresponding region of the Rabex-5 HB-Vps9 tandem prevents soluble expression. Impaired exchange activity resulting from mutation of a conserved leucine residue in ALS2 is an indirect consequence of its buried location in the hydrophobic core (Otomo et al., 2003). Conversely, loss of exchange activity resulting from mutation of a conserved proline residue in ALS2 likely reflects its partially exposed location within the exchange epitope.

nonnative sequence (Figure 6). It is clear that the 4844ΔT SNP disrupts the structure of the Vps9 domain, eliminating Rab interaction determinants and exposing many nonpolar residues otherwise buried in the hydrophobic core. Furthermore, the frame-shifted sequence following 4844ΔT encodes a high percentage of nonpolar residues, which likely exacerbates the severity of the structural defect. In RIN1, a splice variant that deletes the region from the N terminus of αHB4 to the N terminus of αV2 fails to interact with Rab5 in a two-hybrid assay (Tall et al., 2001). This region contains the conserved/buried acidic residues required for the structural stability and soluble expression of the Rabex-5 HB-Vps9 tandem. Thus, the inability of the RIN1 splice variant to interact with Rab5 likely results from a structural defect rather than the loss of critical exchange determinants.

Discussion

In addition to structural evidence, the lack of soluble expression for either the isolated Vps9 domain or the E212A mutant at the HB-Vps9 domain interface supports the conclusion that the HB and Vps9 domains function as an integrated tandem. Several observations suggest that an analogous tandem architecture is likely to be a general feature of Vps9 domain proteins. First, the residues in the Vps9 domain that contact the helical bundle are conserved. Second, the sequences of Vps9 domain proteins encode at least four predicted helices N-terminal to the Vps9 domain. Third, the level of sequence conservation in the helical bundle is strongly correlated with the degree to which residues are buried in the Rabex-5 structure. Finally, a construct of RIN1 corresponding to the HB-Vps9 tandem of Rabex-5 can be expressed in a soluble form and has comparable catalytic activity and Rab specificity (data not shown). Moreover, a splice-variant of RIN1, which deletes the region from the N terminus of αN4 to the N terminus of αV2, fails to interact with a dominant-negative mutant of Rab5 in a yeast two-hybrid assay, as does a construct that begins at the N terminus of αV1 and extends through the C terminus of the protein (Tall et al., 2001).

A tandem architecture has also been observed in other GEFs. For example, the Sos protein contains two GEF activities, a DH-PH tandem that functions as a Rac GEF, and a Ras GEF tandem consisting of a N-terminal helical domain and the core catalytic domain (Boriack-Sjodin et al., 1998; Margarit et al., 2003; Nimnual et al., 1998). In the latter case, GTP bound Ras stimulates the exchange activity by binding at the interface between the two domains and inducing a conformational change that allows the N-terminal domain to contribute to the interaction with nucleotide free Ras (Margarit et al., 2003). The DH-PH tandem of Rho family GEFs exhibits considerable variability in the arrangement of the DH and PH domains (Rossman et al., 2002a, 2002b; Snyder et al., 2002; Soisson et al., 1998; Worthylake et al., 2000). In one instance, the PH domain contacts the GTPase and contributes directly to exchange activity (Rossman et al., 2003, 2002b). In Rabex-5, the surface of the helical bundle is poorly conserved, suggesting that it does not generally mediate direct interactions with Rab GTPases. Nevertheless, the helical bundle does contribute indirectly to exchange activity by stabilizing the Vps9 domain. Beyond a structural role, it is possible that the helical bundle may play a role in allosteric regulation, which has been observed in RIN1 (Tall et al., 2001).

An investigation of the catalytic properties of full-length Rabex-5 and Vps9p concluded that these proteins are weak exchangers compared with other well-characterized GEFs, in particular RCC1 and EF-Ts, which catalyze exchange for Ran and EF-Tu, respectively (Esters et al., 2001). The exchange rate for full-length Rabex-5 saturates in the nM concentration range ($K_m = 270$ nM) with a k_{cat} of 0.007 s^{-1}. We also observe equivalently weak exchange activity for full-length Rabex-5. For the HB-Vps9 tandem, on the other hand, $K_m > 2$ μM and $k_{cat} > 0.1$ s^{-1}. One possible explanation is that the low catalytic activity of full-length Rabex-5 reflects improper folding of one or more domains in the bacterially expressed protein. In support of this view, Rabex-5 has higher exchange activity in the complex with Rabaptin-5 (Lippe et al., 2001). An alternative hypothesis is that the lower exchange activity reflects autoinhibition by regulatory elements in the regions N- and/or C-terminal to the HB-Vps9 tandem. In this case, the interac-

tion of GTP bound Rab5 with Rabaptin-5 might stimulate the exchange activity of the HB-Vps9 tandem, in addition to recruiting Rabex-5 to membranes. Additional experiments are necessary to distinguish between these possibilities.

Little is currently known about Rab21, although it is reported to have a relatively broad tissue distribution and to localize to the endoplasmic reticulum (ER) in unpolarized epithelial cells and to an apical pool of vesicles in polarized cells (Opdam et al., 2000). Rab22 localizes to endosomes as well as the trans Golgi network (TGN) and is proposed to regulate transport between the TGN and endosomes (Kauppi et al., 2002; Mesa et al., 2001; Rodriguez-Gabin et al., 2001). Interestingly, the N terminus of EEA1 binds Rab22 as well as Rab5, suggesting a potential molecular mechanism for regulating the fusion of endosomes with vesicles derived from the TGN (Kauppi et al., 2002). Furthermore, the Rabaptin-5-Rabex-5 complex interacts with GGA proteins, which associate with the TGN and function as Arf-dependent clathrin adaptors (Mattera et al., 2003). One possibility is that GGA-dependent recruitment of the Rabaptin-5-Rabex-5 complex to the TGN leads to activation of Rab22, which may in turn be required for the fusion of TGN-derived vesicles with endosomes. This would be plausible if the weak exchange activity for Rab22 reflects a high K_m rather than a low k_{cat}, in which case locally high concentrations resulting from colocalization might overcome a low affinity for Rab22. Additional studies will be required to characterize the Rab specificity of the other proteins that contain Vps9 domains and determine whether these proteins and/or the Rabaptin-5-Rabex-5 complex function as Rab21 and/or Rab22 GEFs in vivo.

Since the *ALS2* gene was cloned, 9 SNPs from different families have been identified throughout the coding region (Devon et al., 2003; Eymard-Pierre et al., 2002; Gros-Louis et al., 2003; Hadano et al., 2001; Yang et al., 2001). All of the SNPs involve frame shift or non-sense mutations that result in C-terminal truncations, the clinical severity of which does not correlate with the extent of the truncation (Devon et al., 2003). Given that the truncated protein products lack part or all of the Vps9 domain, it has been suggested that the motor neuron degeneration associated with the *ALS2* SNPs might result from loss of Rab5 GEF activity (Otomo et al., 2003). However, the various *ALS2* SNPs, including that in the Vps9 domain, give rise to unstable proteins that are targeted for degradation (Yamanaka et al., 2003). From the structural and functional data presented here, it is clear that the SNP in the Vps9 domain necessarily results in a major structural defect in addition to eliminating critical determinants of GEF activity. The identification of point mutants that severely impair GEF activity without apparent effect on the structure of the Rabex-5 HB-Vps9 domain tandem should provide useful reagents for exploring the in vivo consequences resulting from impaired GEF activity in ALS2 as well as other proteins that contain Vps9 domains.

Experimental Procedures

Constructs
Constructs were amplified with Vent polymerase (New England Biolabs) and sequenced to ensure the absence of mutations. Human Rabex-5 constructs were subcloned into a modified pET15b vector containing an N-terminal His$_6$ tag (MGHHHHHGS). Rab GTPases (Supplemental Table 1 available on *Cell* website) were subcloned into PGEX-4T1 (Pharmacia), which provides an N-terminal GST tag followed by a thrombin site. Rab8, Rab10, and Rab17 were subcloned into the pET44a vector (Novagen), which incorporates an N-terminal fusion containing a 6xHis tag, the NusA protein, and a thrombin site. Site-specific mutants were generated using the QuickChange kit (Stratagene).

Expression and Purification
BL21(DE3)-RIL cells (Stratagene) transformed with expression vectors containing Rab or Rabex-5 constructs were grown at 20°C in 2xYT with 100 mg/L ampicillin to an OD$_{600}$ of 0.2 and induced with 0.05 mM IPTG for 16 hr. Cells were resuspended in 50 mM Tris, 50 mM NaCl, and 0.1% β-mercaptoethanol (β-ME), disrupted by sonication, and centrifuged for 40 min at 35000g. For 6xHis fusion proteins, the supernatants were loaded onto Ni-NTA agarose columns (Qiagen) and washed with 50 mM Tris, [pH 8.5], 500 mM NaCl, 10 mM imidazole, and 0.1% β-ME (Buffer A). The 6xHis fusion proteins were eluted with a gradient of 10–150 mM imidazole in 50 mM Tris, [pH 8.5], 150 mM NaCl, and 0.1% β-ME (Buffer B). For GST fusion proteins, the supernatants were loaded onto glutathione-Sepharose columns (Amersham) and washed with Buffer A. GST fusion proteins were eluted with 10 mM glutathione in Buffer B. For Rab proteins, all buffers were supplemented with 0.5 mM MgCl$_2$. Wild-type Rabex-5 constructs were further purified by anion exchange chromatography over Source Q (Amersham) and gel filtration chromatography over Superdex-75 (Amersham).

Crystallization and Structure Determination
Crystals of selenomethionine-substituted Rabex-5$_{132-394}$ were grown at 4°C in hanging drops containing 12 mg/ml protein in 30% PEG 8000, 450 mM MgCl$_2$, and 50 mM Tris, [pH 8.0]. Crystals appeared in 2–3 days and grew to maximum dimensions of 0.05 × 0.1 × 0.2 mm over 2 weeks. The crystals are in the space group P2$_1$2$_1$2 with unit cell dimensions a = 68.0 Å, b = 88.3 Å, c = 47.3 Å, one molecule in the asymmetric unit, and a solvent content of 43%. Crystals were transferred to a cryostabilizer (30% PEG 8000, 50 mM Tris, [pH 8.0], 450 mM MgCl$_2$ 10% glycerol), frozen in liquid propane, and maintained at 100°K in a nitrogen cryostream. The structure was solved by multiwavelength anomalous diffraction at the selenium edge. Data were collected at the X12B beam line at the National Synchrotron Light Source using an inverse beam strategy. Data were collected on two isomorphous crystals at the f″ maximum, f′ minimum, and high as well as low energy remote wavelengths (Table 1). Data were processed with Denzo and scaled with Scalepack (Otwinowski and Minor, 1997). Nine Se sites were identified by Patterson and direct methods (SHELXS) using the Bijvoet differences at the f″ maximum. The heavy atom model was refined using SHARP (La Fortelle and Bricogne, 1997). Following phase-improvement by solvent flipping with Solomon, a σA-weighted Fourier summation yielded an interpretable map with continuous density for the main chain and most side chains (CCP4, 1994). An initial model constructed with ArpWarp was completed by manual building in O (CCP4, 1994; Jones et al., 1991) and refined against data from 20 to 2.35 Å using simulated annealing and positional refinement in CNS and Refmac5 (Brunger et al., 1998; CCP4, 1994). The refined model, which includes residues 134–387, 82 water molecules, and an ordered Mg^{2+} ion, has an R factor of 22.7% and a free R factor of 26.9% with excellent stereochemistry. The Mg^{2+} ion is coordinated by nonconserved residues and does not have an obvious structural or functional significance. Structural figures were generated with PyMol (http://www.pymol.org).

Nucleotide Exchange Assays
Exchange kinetics were measured by monitoring either the quenching of fluorescence following the release of the nucleotide analog 2′-(3′)-bis-O-(N-methylanthraniloyl)-GDP (mant-GDP, Molecular Probes) or the decrease in intrinsic tryptophan fluorescence accompanying conversion to the active state. For mant-GDP assays, Rab proteins were loaded with mant-GDP as described (Zhu et al., 2001) and diluted to 1.0 μM in 50 mM Tris, [pH 8.0], 150 mM NaCl, and 0.5

mM MgCl$_2$. Samples were excited at 360 nm and the emission monitored at 440 nm. For intrinsic tryptophan fluorescence measurements, Rab5 was diluted to 1.0 μM in 20 mM Tris-HCl, [pH 8.0], 150 mM NaCl, and 0.5 mM MgCl$_2$ and the emission monitored at 340 nm with excitation at 300 nm. For both intrinsic tryptophan and mant-GDP assays, exchange reactions were initiated by addition of 200 μM GppNHp and varying concentrations of Rabex-5$_{132-391}$. Data were collected using a Saphire multimode microplate spectrophotometer (Tecan) or a PC1 spectrofluorimeter (ISS). Observed pseudofirst order rate constants (k$_{obs}$) were extracted from a nonlinear least-squares fit to the exponential function

$$I(t) = (I_0 - I_\infty) \exp(-k_{obs} t) + I_\infty \qquad (1)$$

where I(t) is the emission intensity as a function of time and I$_0$ and I$_\infty$ are the emission intensities at t = 0 and t = ∞, respectively. The catalytic efficiency, k$_{cat}$/K$_m$, was obtained from the slope of a linear least-squares fit to

$$k_{obs} = (k_{cat}/K_m) \, [\text{Rabex-5}] + k_{intr} \qquad (2)$$

where k$_{intr}$ is the intrinsic rate constant for GDP-release in the absence of Rabex-5.

Acknowledgments

References

Afar, D.E., Han, L., McLaughlin, J., Wong, S., Dhaka, A., Parmar, K., Rosenberg, N., Witte, O.N., and Colicelli, J. (1997). Regulation of the oncogenic activity of BCR-ABL by a tightly bound substrate protein RIN1. Immunity 6, 773–782.

Alexandrov, K., Scheidig, A.J., and Goody, R.S. (2001). Fluorescence methods for monitoring interactions of Rab proteins with nucleotides, Rab escort protein, and geranylgeranyltransferase. Methods Enzymol. 329, 14–31.

Bateman, A., Coin, L., Durbin, R., Finn, R.D., Hollich, V., Griffiths-Jones, S., Khanna, A., Marshall, M., Moxon, S., Sonnhammer, E.L., et al. (2004). The Pfam protein families database. Nucleic Acids Res. 32, D138–D141.

Boriack-Sjodin, P.A., Margarit, S.M., Bar-Sagi, D., and Kuriyan, J. (1998). The structural basis of the activation of Ras by Sos. Nature 394, 337–343.

Brunger, A.T., Adams, P.D., Clore, G.M., DeLano, W.L., Gros, P., Grosse-Kunstleve, R.W., Jiang, J.S., Kuszewski, J., Nilges, M., Pannu, N.S., et al. (1998). Crystallography & NMR system: a new software suite for macromolecular structure determination. Acta Crystallogr. D Biol. Crystallogr. 54, 905–921.

Burd, C.G., Mustol, P.A., Schu, P.V., and Emr, S.D. (1996). A yeast protein related to a mammalian Ras-binding protein, Vps9p, is required for localization of vacuolar proteins. Mol. Cell. Biol. 16, 2369–2377.

CCP4 (1994). The CCP4 suite: programs for protein crystallography. Acta Crystallogr. D Biol Crystallogr 50, 760–763.

Cerione, R.A., and Zheng, Y. (1996). The Dbl family of oncogenes. Curr. Opin. Cell Biol. 8, 216–222.

Christoforidis, S., McBride, H.M., Burgoyne, R.D., and Zerial, M. (1999). The Rab5 effector EEA1 is a core component of endosome docking. Nature 397, 621–625.

de Renzis, S., Sonnichsen, B., and Zerial, M. (2002). Divalent Rab effectors regulate the sub-compartment organization and sorting of early endosomes. Nat. Cell Biol. 4, 124–133.

Devon, R.S., Helm, J.R., Rouleau, G.A., Leitner, Y., Lerman-Sagie, T., Lev, D., and Hayden, M.R. (2003). The first nonsense mutation in alsin results in a homogeneous phenotype of infantile-onset ascending spastic paralysis with bulbar involvement in two siblings. Clin. Genet. 64, 210–215.

Dhaka, A., Costa, R.M., Hu, H., Irvin, D.K., Patel, A., Kornblum, H.I., Silva, A.J., ODell, T.J., and Colicelli, J. (2003). The RAS effector RIN1 modulates the formation of aversive memories. J. Neurosci. 23, 748–757.

Esters, H., Alexandrov, K., Iakovenko, A., Ivanova, T., Thoma, N., Rybin, V., Zerial, M., Scheidig, A.J., and Goody, R.S. (2001). Vps9, Rabex-5 and DSS4: proteins with weak but distinct nucleotide-exchange activities for Rab proteins. J. Mol. Biol. 310, 141–156.

Eymard-Pierre, E., Lesca, G., Dollet, S., Santorelli, F.M., di Capua, M., Bertini, E., and Boespflug-Tanguy, O. (2002). Infantile-onset ascending hereditary spastic paralysis is associated with mutations in the alsin gene. Am. J. Hum. Genet. 71, 518–527.

Gournier, H., Stenmark, H., Rybin, V., Lippe, R., and Zerial, M. (1998). Two distinct effectors of the small GTPase Rab5 cooperate in endocytic membrane fusion. EMBO J. 17, 1930–1940.

Gros-Louis, F., Meijer, I.A., Hand, C.K., Dube, M.P., MacGregor, D.L., Seni, M.H., Devon, R.S., Hayden, M.R., Andermann, F., Andermann, E., and Rouleau, G.A. (2003). An ALS2 gene mutation causes hereditary spastic paraplegia in a Pakistani kindred. Ann. Neurol. 53, 144–145.

Hadano, S., Hand, C.K., Osuga, H., Yanagisawa, Y., Otomo, A., Devon, R.S., Miyamoto, N., Showguchi-Miyata, J., Okada, Y., Singaraja, R., et al. (2001). A gene encoding a putative GTPase regulator is mutated in familial amyotrophic lateral sclerosis 2. Nat. Genet. 29, 166–173.

Hama, H., Tall, G.G., and Horazdovsky, B.F. (1999). Vps9p is a guanine nucleotide exchange factor involved in vesicle-mediated vacuolar protein transport. J. Biol. Chem. 274, 15284–15291.

Han, L., Wong, D., Dhaka, A., Afar, D., White, M., Xie, W., Herschman, H., Witte, O., and Colicelli, J. (1997). Protein binding and signaling properties of RIN1 suggest a unique effector function. Proc. Natl. Acad. Sci. USA 94, 4954–4959.

Horiuchi, H., Lippe, R., McBride, H.M., Rubino, M., Woodman, P., Stenmark, H., Rybin, V., Wilm, M., Ashman, K., Mann, M., and Zerial, M. (1997). A novel Rab5 GDP/GTP exchange factor complexed to Rabaptin-5 links nucleotide exchange to effector recruitment and function. Cell 90, 1149–1159.

Jones, T.A., Zou, J.Y., Cowan, S.W., and Kjeldgaard, M. (1991). Improved methods for building protein models in electron density maps and the location of errors in these models. Acta Crystallogr. A 47, 110–119.

Kajiho, H., Saito, K., Tsujita, K., Kontani, K., Araki, Y., Kurosu, H., and Katada, T. (2003). RIN3: a novel Rab5 GEF interacting with amphiphysin II involved in the early endocytic pathway. J. Cell Sci. 116, 4159–4168.

Kauppi, M., Simonsen, A., Bremnes, B., Vieira, A., Callaghan, J., Stenmark, H., and Olkkonen, V.M. (2002). The small GTPase Rab22 interacts with EEA1 and controls endosomal membrane trafficking. J. Cell Sci. 115, 899–911.

La Fortelle, E.D., and Bricogne, G. (1997). Maximum-likelihood heavy-atom parameter refinement for the multiple isomorphous replacement and multiwavelength anomalous diffraction methods. Methods Enzymol. 276, 472–494.

Letunic, I., Copley, R.R., Schmidt, S., Ciccarelli, F.D., Doerks, T., Schultz, J., Ponting, C.P., and Bork, P. (2004). SMART 4.0: towards genomic data integration. Nucleic Acids Res. 32, D142–D144.

Lippe, R., Miaczynska, M., Rybin, V., Runge, A., and Zerial, M. (2001). Functional synergy between Rab5 effector Rabaptin-5 and exchange factor Rabex-5 when physically associated in a complex. Mol. Biol. Cell 12, 2219–2228.

Macia, E., Chabre, M., and Franco, M. (2001). Specificities for the small G proteins ARF1 and ARF6 of the guanine nucleotide exchange factors ARNO and EFA6. J. Biol. Chem. 276, 24925–24930.

Margarit, S.M., Sondermann, H., Hall, B.E., Nagar, B., Hoelz, A.,

Pirruccello, M., Bar-Sagi, D., and Kuriyan, J. (2003). Structural evidence for feedback activation by Ras.GTP of the Ras-specific nucleotide exchange factor SOS. Cell 112, 685–695.

Mattera, R., Arighi, C.N., Lodge, R., Zerial, M., and Bonifacino, J.S. (2003). Divalent interaction of the GGAs with the Rabaptin-5-Rabex-5 complex. EMBO J. 22, 78–88.

McBride, H.M., Rybin, V., Murphy, C., Giner, A., Teasdale, R., and Zerial, M. (1999). Oligomeric complexes link Rab5 effectors with NSF and drive membrane fusion via interactions between EEA1 and syntaxin 13. Cell 98, 377–386.

Merithew, E., Stone, C., Eathiraj, S., and Lambright, D.G. (2003). Determinants of Rab5 interaction with the N terminus of early endosome antigen 1. J. Biol. Chem. 278, 8494–8500.

Mesa, R., Salomon, C., Roggero, M., Stahl, P.D., and Mayorga, L.S. (2001). Rab22a affects the morphology and function of the endocytic pathway. J. Cell Sci. 114, 4041–4049.

Mills, I.G., Jones, A.T., and Clague, M.J. (1998). Involvement of the endosomal autoantigen EEA1 in homotypic fusion of early endosomes. Curr. Biol. 8, 881–884.

Mossessova, E., Gulbis, J.M., and Goldberg, J. (1998). Structure of the guanine nucleotide exchange factor Sec7 domain of human arno and analysis of the interaction with ARF GTPase. Cell 92, 415–423.

Mossessova, E., Corpina, R.A., and Goldberg, J. (2003). Crystal structure of ARF1*Sec7 complexed with Brefeldin A and its implications for the guanine nucleotide exchange mechanism. Mol. Cell 12, 1403–1411.

Nielsen, E., Christoforidis, S., Uttenweiler-Joseph, S., Miaczynska, M., Dewitte, F., Wilm, M., Hoflack, B., and Zerial, M. (2000). Rabenosyn-5, a novel Rab5 effector, is complexed with hVPS45 and recruited to endosomes through a FYVE finger domain. J. Cell Biol. 151, 601–612.

Nimnual, A.S., Yatsula, B.A., and Bar-Sagi, D. (1998). Coupling of Ras and Rac guanosine triphosphatases through the Ras exchanger Sos. Science 279, 560–563.

Nuoffer, C., Wu, S.K., Dascher, C., and Balch, W.E. (1997). Mss4 does not function as an exchange factor for Rab in endoplasmic reticulum to Golgi transport. Mol. Biol. Cell 8, 1305–1316.

Opdam, F.J., Kamps, G., Croes, H., van Bokhoven, H., Ginsel, L.A., and Fransen, J.A. (2000). Expression of Rab small GTPases in epithelial Caco-2 cells: Rab21 is an apically located GTP-binding protein in polarised intestinal epithelial cells. Eur. J. Cell Biol. 79, 308–316.

Otomo, A., Hadano, S., Okada, T., Mizumura, H., Kunita, R., Nishijima, H., Showguchi-Miyata, J., Yanagisawa, Y., Kohiki, E., Suga, E., et al. (2003). ALS2, a novel guanine nucleotide exchange factor for the small GTPase Rab5, is implicated in endosomal dynamics. Hum. Mol. Genet. 12, 1671–1687.

Otwinowski, Z., and Minor, W. (1997). Processing of X-ray Diffraction Data Collected in Oscillation Mode. Methods Enzymol. 276, 307–326.

Pereira-Leal, J.B., and Seabra, M.C. (2000). The mammalian Rab family of small GTPases: definition of family and subfamily sequence motifs suggests a mechanism for functional specificity in the Ras superfamily. J. Mol. Biol. 301, 1077–1087.

Pereira-Leal, J.B., and Seabra, M.C. (2001). Evolution of the Rab family of small GTP-binding proteins. J. Mol. Biol. 313, 889–901.

Pfeffer, S.R. (2001). Rab GTPases: specifying and deciphering organelle identity and function. Trends Cell Biol. 11, 487–491.

Renault, L., Guibert, B., and Cherfils, J. (2003). Structural snapshots of the mechanism and inhibition of a guanine nucleotide exchange factor. Nature 426, 525–530.

Rodriguez-Gabin, A.G., Cammer, M., Almazan, G., Charron, M., and Larocca, J.N. (2001). Role of rRAB22b, an oligodendrocyte protein, in regulation of transport of vesicles from trans Golgi to endocytic compartments. J. Neurosci. Res. 66, 1149–1160.

Rossman, K.L., Worthylake, D.K., Snyder, J.T., Cheng, L., Whitehead, I.P., and Sondek, J. (2002a). Functional analysis of cdc42 residues required for Guanine nucleotide exchange. J. Biol. Chem. 277, 50893–50898.

Rossman, K.L., Worthylake, D.K., Snyder, J.T., Siderovski, D.P.,

Campbell, S.L., and Sondek, J. (2002b). A crystallographic view of interactions between Dbs and Cdc42: PH domain-assisted guanine nucleotide exchange. EMBO J. 21, 1315–1326.

Rossman, K.L., Cheng, L., Mahon, G.M., Rojas, R.J., Snyder, J.T., Whitehead, I.P., and Sondek, J. (2003). Multifunctional roles for the PH domain of Dbs in regulating Rho GTPase activation. J. Biol. Chem. 278, 18393–18400.

Segev, N. (2001). Ypt and Rab GTPases: insight into functions through novel interactions. Curr. Opin. Cell Biol. 13, 500–511.

Simon, I., Zerial, M., and Goody, R.S. (1996). Kinetics of interaction of Rab5 and Rab7 with nucleotides and magnesium ions. J. Biol. Chem. 271, 20470–20478.

Simonsen, A., Lippe, R., Christoforidis, S., Gaullier, J.M., Brech, A., Callaghan, J., Toh, B.H., Murphy, C., Zerial, M., and Stenmark, H. (1998). EEA1 links PI(3)K function to Rab5 regulation of endosome fusion. Nature 394, 494–498.

Snyder, J.T., Worthylake, D.K., Rossman, K.L., Betts, L., Pruitt, W.M., Siderovski, D.P., Der, C.J., and Sondek, J. (2002). Structural basis for the selective activation of Rho GTPases by Dbl exchange factors. Nat. Struct. Biol. 9, 468–475.

Soisson, S.M., Nimnual, A.S., Uy, M., Bar-Sagi, D., and Kuriyan, J. (1998). Crystal structure of the Dbl and pleckstrin homology domains from the human Son of sevenless protein. Cell 95, 259–268.

Stenmark, H., Vitale, G., Ullrich, O., and Zerial, M. (1995). Rabaptin-5 is a direct effector of the small GTPase Rab5 in endocytic membrane fusion. Cell 83, 423–432.

Tall, G.G., Barbieri, M.A., Stahl, P.D., and Horazdovsky, B.F. (2001). Ras-activated endocytosis is mediated by the Rab5 guanine nucleotide exchange activity of RIN1. Dev. Cell 1, 73–82.

Wang, Y., Waldron, R.T., Dhaka, A., Patel, A., Riley, M.M., Rozengurt, E., and Colicelli, J. (2002). The RAS effector RIN1 directly competes with RAF and is regulated by 14-3-3 proteins. Mol. Cell. Biol. 22, 916–926.

Whitehead, I.P., Campbell, S., Rossman, K.L., and Der, C.J. (1997). Dbl family proteins. Biochim. Biophys. Acta 1332, F1–23.

Worthylake, D.K., Rossman, K.L., and Sondek, J. (2000). Crystal structure of Rac1 in complex with the guanine nucleotide exchange region of Tiam1. Nature 408, 682–688.

Yamanaka, K., Vande Velde, C., Eymard-Pierre, E., Bertini, E., Boespflug-Tanguy, O., and Cleveland, D.W. (2003). Unstable mutants in the peripheral endosomal membrane component ALS2 cause early-onset motor neuron disease. Proc. Natl. Acad. Sci. USA 100, 16041–16046.

Yang, Y., Hentati, A., Deng, H.X., Dabbagh, O., Sasaki, T., Hirano, M., Hung, W.Y., Ouahchi, K., Yan, J., Azim, A.C., et al. (2001). The gene encoding alsin, a protein with three guanine-nucleotide exchange factor domains, is mutated in a form of recessive amyotrophic lateral sclerosis. Nat. Genet. 29, 160–165.

Zerial, M., and McBride, H. (2001). Rab proteins as membrane organizers. Nat. Rev. Mol. Cell Biol. 2, 107–117.

Zhu, Z., Dumas, J.J., Lietzke, S.E., and Lambright, D.G. (2001). A helical turn motif in Mss4 is a critical determinant of Rab binding and nucleotide release. Biochemistry 40, 3027–3036.

Accession Numbers

Coordinates have been deposited with the Protein Data Bank under the ID code 1TXU.